Dalton Transactions

ROYAL SOCIETY OF CHEMISTRY

PAPER

View Article Online
View Journal | View Issue

Cite this: *Dalton Trans.*, 2022, **51**, 4843

Enantiopure and racemic radical-cation salts of B(mandelate)$_2^-$ and B(2-chloromandelate)$_2^-$ anions with BEDT-TTF†

Toby J. Blundell, [a] Jordan R. Lopez,[a] Kathryn Sneade,[a] John D. Wallis, [a] Hiroki Akutsu, [b] Yasuhiro Nakazawa,[b] Simon J. Coles, [c] Claire Wilson [c] and Lee Martin *[a]

Received 4th January 2022,
Accepted 28th February 2022

DOI: 10.1039/d2dt00024e

rsc.li/dalton

We report the first examples of radical-cation salts of BEDT-TTF with spiroborate anions [B(mandelate)$_2$]$^-$ and [B(2-chloromandelate)$_2$]$^-$, synthesized from either enantiopure or racemic bidentate mandelate or chloromandelate ligands. In the salts prepared using enantiopure ligands only one of two diastereoisomers of the spiroborate anion is incorporated, with the boron centre having the same stereochemistry as the enantiopure ligand. For the racemic salts one racemic pair of spiroborate anions containing an *R* and an *S* mandelate ligand is incorporated. In certain solvents helical crystals were obtained when using spiroborate anions with enantiopure ligands. Electrical and magnetic properties, and band structure calculations are reported.

Introduction

The pursuit of materials containing more than one physical property *via* crystal engineering has garnered much interest over recent years. Bis(ethylenedithio)tetrathiafulvalene (BEDT-TTF) radical-cation salts have been shown as promising candidates for such materials in producing crystals combining properties such as chirality and conductivity.[1] By altering the conducting BEDT-TTF layers and insulating anion layers it is possible to tailor multiple physical properties in a single material.[2] Electrical magneto-chiral anisotropy (EMChA), where the resistivity of materials of opposite chiral enantiomers differs, has been observed in bismuth helices[3] and carbon nanotubes.[4] More recently, Pop *et al.* observed EMChA in the radical-cation salts of (*S*,*S*)- and (*R*,*R*)-(DM-EDT-TTF)$_2$ClO$_4$.[5] Crystallising in the chiral space groups $P6_122$ and $P6_422$, metallic behaviour was observed down to 40 K confirming the chiral nature of charge transport. However, synthesising the analogous enantiopure salts with the PF_6 anion resulted in charge ordered semiconducting behavior, or when racemic DM-EDT-TTF was used, metal like conductivity.[6]

There are three routes whereby chirality can be introduced into radical-cation salts: a chiral donor, chiral anion/acceptor or by the use of a chiral solvent. Since the first chiral TTF-based donor molecule tetramethyl-(*S*,*S*,*S*,*S*)-BEDT-TTF was synthesised[7] a large number of enantiopure TTF-based compounds have been reported including hydroxyalkyl-BEDT-TTFs,[8] bis(oxazoline)-TTFs,[9] iodo-TTFs,[10] pyrrolo-TTFs[11] and TTF-sulphoxides which contain chiral sulphur atoms.[12] Recently a semiconducting TTF-type donor was observed to show a lower activation energy for the racemic salt as compared to the enantiopure analogues.[13] A chiral molecular conductor of (1′*R*,5*S*)-*N*-(1′-phenylethyl)(BEDT-TTF)acetamide with TCNQ which remains metallic down to 4.2 K was recently reported.[14] This salt also exhibits room-temperature switching capabilities with a transition to an insulating state above 10 °C.[14]

Enantiopure chiral anions, as well as their racemic mixtures, have also been utilised in the synthesis of radical-cation salts with BEDT-TTF including Fe(croconate)$_3$,[15] Cr(2,2′-bipy)(oxalate)$_2$,[16] Sb$_2$(L-tartrate)$_2$,[17] TRISPHAT[18] and Fe(C$_6$O$_4$Cl$_2$)$_3$[19] with the latter also combining with chiral TM-BEDT-TTF in the synthesis of a rare example incorporating both a chiral donor and anion molecules in a single salt although the anion crystallised as a racemic mixture.[20] An enantiopure bishydroxy-substituted TTF donor has also produced a 4 : 1 salt with the *meso* stereoisomer of the dinuclear [Fe$_2$(oxalate)$_5$]$^{4-}$ anion.[21]

The most widely reported family of chiral anions with BEDT-TTF salts is that of the tris(oxalato)metallates which have provided a wide array of materials combining magnetism and conductivity in the same material.[22] These compounds contain a mixture of the Δ and Λ isomers of [M(oxalate)$_3$]$^{3-}$ resulting in a racemic solid-state lattice and the spatial distri-

[a]*School of Science and Technology, Nottingham Trent University, Clifton Lane, Clifton, Nottingham, NG11 8NS, UK. E-mail: lee.martin@ntu.ac.uk; Tel: +44 (0)1158483128*
[b]*Department of Chemistry, Graduate School of Science, Osaka University, 1-1 Machikaneyama-cho, Toyonaka, Osaka 560-0043, Japan*
[c]*School of Chemistry, Faculty of Natural and Environmental Sciences, University of Southampton, Highfield, Southampton, SO17 1BJ, UK*

†Electronic supplementary information (ESI) available. CCDC 2129470 and 2129471 for **I** and **III**. For ESI and crystallographic data in CIF or other electronic format see DOI: 10.1039/d2dt00024e

bution of these layers determines the crystal packing arrangement and *ergo* the conducting properties.[23]

The synthesis of bis-chelated spiroborate anions produces complexes with more than one stereogenic centre. The chirality of the bidentate chelated ligand is retained but diastereomers are produced through two possible stereochemical configurations at the boron centre, which is labile in solution. Therefore, when using enantiopure *R* bidentate ligands, a pair of diastereoisomeric anions will be produced in solution: B_SRR with an *S* boron centre and two *R* bidentate ligands, and B_RRR which differs only in having an *R* boron centre (Scheme 1). When using a racemic bidentate ligand four further diastereomers are obtained: B_SSS and B_RSS (the mirror images of the anions shown in Scheme 1) and B_SRS and B_RRS (Scheme 2).

We previously reported radical-cation salts of BEDT-TTF with spiroborate anions of malic acid.[24] Crystals grown electrochemically in the presence of a mixture of B_SRR and B_RRR anions (produced from enantiopure *R*-(−)-malic acid) gave a chiral radical-cation salt in which only the B_SRR anion was incorporated into the structure. When using a mixture of the six possible diastereomeric spiroborate anions prepared from racemic malic acid, a racemic radical-cation salt was obtained but only two of the six diastereomeric anions were present in the crystal (B_SRS and B_RRS).[24]

We report here the first BEDT-TTF radical-cation salts incorporating the anions B(mandelate)$_2^-$ and B(2-chloromandelate)$_2^-$ synthesised using either racemic or enantiopure mandelic acids. The chiral B(mandelate)$_2^-$ anions have previously been studied for their chiral resolution and chiral co-crystallisation abilities.[25] These properties can be attributed to the different shapes that are adopted depending on whether the boron centre is in the *S* or *R* configuration. For instance, the B_RRR anion adopts a 'V' shape and the B_SRR anion adopts a planar 'twist' (Fig. 1). The same holds true also for the B_SSS ('V') and the B_RSS ('twist') anions. It has been suggested that the 'V' shaped anion has fewer packing modes available for crystallisation when compared with the more planar 'twisted' anion.[25]

Scheme 1 The two spiroborate anions which can be formed using *R*-mandelic acid differing in chirality at the boron centre.

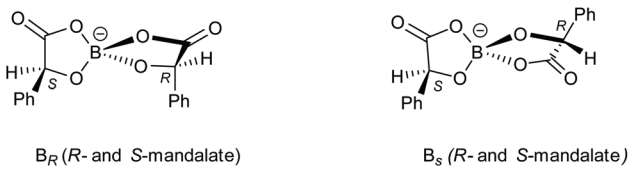

Scheme 2 Spiroborate anions containing a mixture of *R*- and *S*-mandelate enantiomers with either an *R* or *S* boron centre.

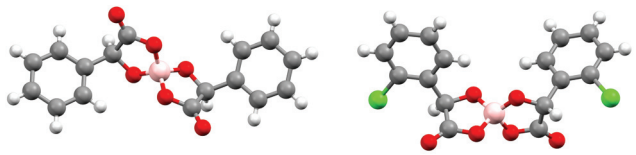

Fig. 1 The twisted (left, B_S(*R*-mandelate)$_2^-$) and 'V' shape (right, B_R(*R*-2-chloromandelate)$_2^-$) spiroborate anions.

We recently reported the first example of a chiral BDH-TTP salt, κ-BDH-TTP$_2$[B_S-(*S*-ClMan)$_2$] (ClMan = 2-(2-chlorophenyl)-2-oxidoacetate).[26] This salt incorporates the enantiopure B(2-chloromandelate)$_2^-$ anion and shows metallic behaviour down to at least 4.2 K which is the lowest temperature at which metallic behaviour has been observed in a chiral molecular radical-cation salt.

In the present contribution, with BEDT-TTF as the donor molecule when using a mixture of the six possible diastereomeric spiroborate anions, prepared from racemic mandelic acid, we obtain a racemic radical-cation salt containing only B_SRR and B_RSS (**I**). Using chiral B(*S*-mandelate)$_2^-$ produced helical crystals (**II**). Using enantiopure *R*- or *S*-2-chloromandelate spiroborate salts in 1,1,2-trichloroethane gave chiral radical-cation salts (**III**) and (**IV**), respectively. Despite repeated attempts under several electrocrystallisation conditions racemic B(2-chloromandelate)$_2^-$ gave no suitable crystals with BEDT-TTF. The inability to obtain crystals from the racemic mixture of B(2-chloromandelate)$_2^-$ could be as a result of the incompatibility in crystallisation of the 'V' and 'twist' anions in the solid state.‡

Results and discussion

β″-(BEDT-TTF)$_2$B$_{R/S}$[(*R*/*S*)-mandelate]$_2$ (I)

Radical-cation salt **I** was synthesised by electrocrystallisation of BEDT-TTF in chlorobenzene containing 18-crown-6 and the mixture of potassium spiroborate salts prepared from racemic mandelic acid. Salt **I** has the formula β-(BEDT-TTF)$_2$B$_{R/S}$[(*R*/*S*)-mandelate]$_2$ and crystallises in the triclinic crystal system in the centrosymmetric space group $P\bar{1}$. The asymmetric unit con-

‡ *Crystal data*: **I**: $C_{36}H_{28}O_6S_{16}B_1$, M = 1080.35, black plate, a = 8.5373(11), b = 11.7643(14), c = 21.647(3) Å, α = 93.708(7), β = 96.881(7), γ = 104.635(7)°, U = 2078.2(5) Å^3, T = 100(2) K, space group $P\bar{1}$, Z = 2, μ = 0.880 mm^{-1}, reflections collected = 21083, independent reflections = 7146, R_1 = 0.0750, wR_2 = 0.1388 [$F^2 > 2\sigma(F^2)$], R_1 = 0.1158, wR_2 = 0.1572 (all data). *Crystal data*: **III**: $C_{40}H_{32}BCl_8O_6S_{16}$, M = 1416.02, gold needle, a = 54.965(2), b = 15.0756(10), c = 6.5340(4), $\alpha = \beta = \gamma$ = 90°, U = 5414.3(5), T = 150(2) K, space group $P2_12_12$, Z = 4, μ = 9.968 mm^{-1}, reflections collected = 23 321, independent reflections = 9312, R_1 = 0.0540, wR_2 = 0.1002 [$I \geq 2\sigma(I)$], R_1 = 0.0810, wR_2 = 0.1114 (all data). Data for **I** were collected on a Rigaku AFC12 goniometer equipped with an enhanced sensitivity (HG) Saturn724+ detector mounted at the window of an FR-E + SuperBright molybdenum rotating anode generator with VHF Varimax optics (70 μm focus). Data for **III** were collected on a Rigaku Oxford Diffraction Xcalibur System equipped with a Sapphire detector at room temperature using MoKα radiation (λ = 0.71073 Å) with the Crysalis software.[30]

sists of two crystallographically independent BEDT-TTF molecules and one spiroborate anion (Fig. 2). The unit cell contains only two of the six diastereomers possible, B_SRR and B_RSS, which differ in their chirality at the boron centre and also differ in the chirality of the mandelate ligands. The other four diastereomers, B_SSS, B_RRR, B_RRS and B_SRS are not present in the crystal lattice in **I**.

We previously reported the first example of diastereomeric induction within the electrocrystallisation environment without the need for external auxiliaries. Using the racemic anion $B(malate)_2^-$ produced a salt with BEDT-TTF where only the B_SRS and B_RRS racemic pair were included in the crystal.[24] Prior to this chiral radical-cation salts had only been synthesised from enantiopure anions,[16,17] or from racemates which have been resolved by using chiral solvents for crystal growth.[22]

The donors stack in the *ab* plane with neighbouring stacks separated in the *c* direction by the anion layer (Fig. 3 and 4). The two independent donors A and B alternate within an ABABABAB stack along the *a* direction. The independent donors alternate AABBAABB in the *b* direction within adjacent stacks. This corresponds to the β″-type packing arrangement of BEDT-TTF donors (Fig. 5). Both terminal ethylene groups are in the twisted eclipsed confirmation with all sp3 carbons displaced equidistant from the TTF core. The two donors each have side-to-side S···S contacts below the sum of van der Waals radii (Table 1).

A double stack arrangement is observed in the anion layer (Fig. 4), where only one diastereoisomer is present in a single stack with the neighbouring stack in the *c* direction consisting of the opposite enantiomer (Fig. 6). There is a network of hydrogen bonding within each stack of anions but there are no intermolecular contacts between neighbouring stacks. Each anion makes three hydrogen bonds with neighbouring anions and there is hydrogen bonding between anions and BEDT-TTF molecules. One carbonyl oxygen makes three hydrogen bonds, two with separate phenyl ring hydrogens of a neighbouring anion [O5B···C14, 3.531(7) Å (H14B, 2.70 Å) and O5B···C7, 3.542(5) Å (H7B, 2.59 Å)] and one with a donor ethylene hydrogen [O5B···C2, 3.238(6) Å (H2A, 2.41 Å)]. One ring O atom

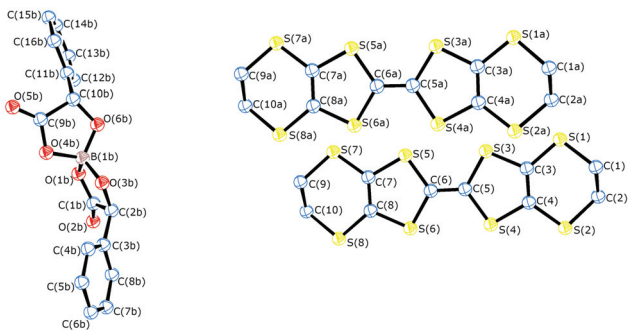

Fig. 2 Asymmetric unit of **I**. Hydrogens omitted for clarity, thermal ellipsoids set at 50% probability.

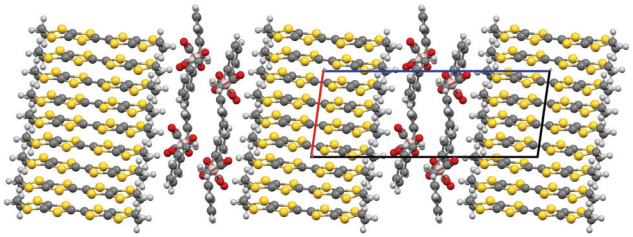

Fig. 3 Layered structure of **I** viewed down the *b* axis.

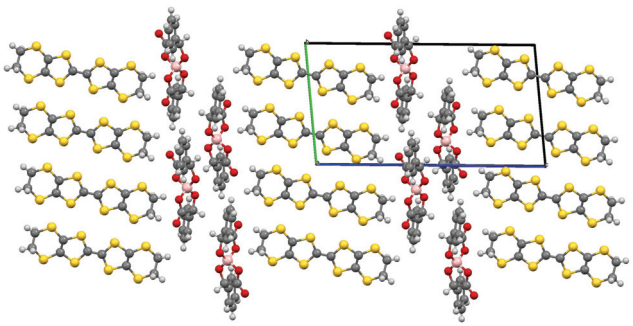

Fig. 4 Layered structure of **I** viewed down the *a* axis.

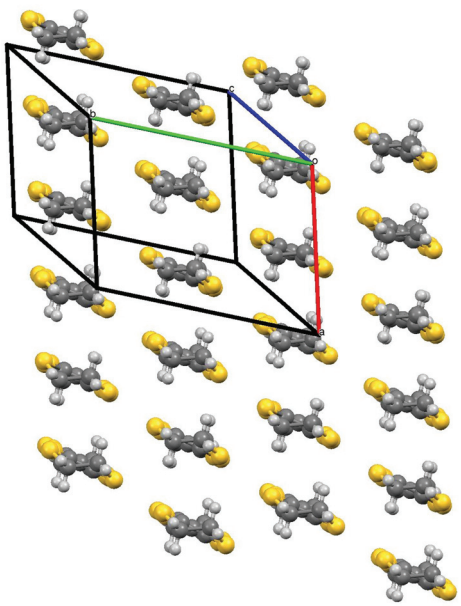

Fig. 5 Donor packing in **I**.

makes a hydrogen bond with a phenyl ring hydrogen [O1B···C5, 3.604(6) (H5B, 2.67 Å)], the same ring O atom also makes a hydrogen bond with a donor ethylene hydrogen [O1B···C10, 3.044(6) Å (H10C, 2.60 Å)].

The molecular formula suggests that the two independent donors have a cumulative charge of +1 to balance the charge of the $B_{R/S}[(R/S)\text{-mandelate}]_2^-$ anion. Using the method of Guionneau *et al.*[27] for estimating oxidation state from mole-

Table 1 S···S contacts shorter than the van der Waals distance for **I**

S···S	Contact/Å
S1···S7	3.450(2)
S3···S7	3.478(19)
S2···S8	3.584(17)
S6···S7A	3.442(18)
S8···S7A	3.386(18)
S2A···S6A	3.431(18)
S2A···S8A	3.399(19)

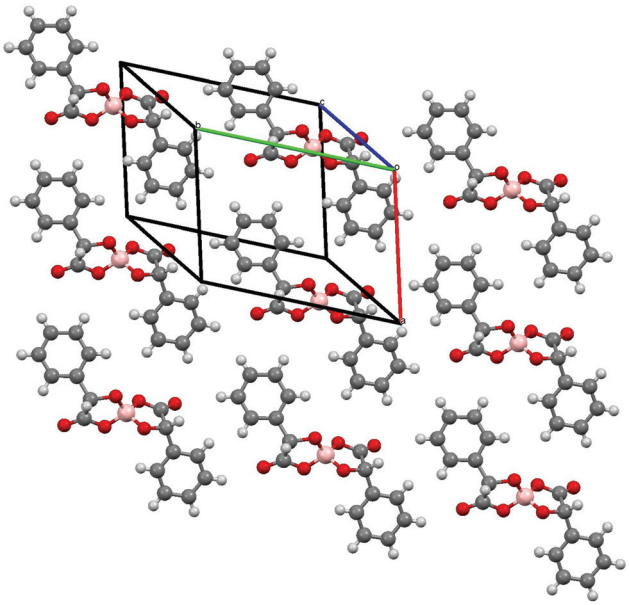

Fig. 6 Anion layer in **I**.

cular geometry the two donors are calculated to each have a charge in the region of 0.5^+ (Table 2). The central C=C bonds are similar in length at 1.368(6) and 1.367(6) Å for independent A and B donors.

The resistivity of **I** is shown in Fig. 7. The activation energy determined from 300 to 200 K is 0.044 eV. Band structure cal-

Table 2 Average bond lengths and estimation of charge on the BEDT-TTF molecules of **I** and **III**. $\delta = (b + c) - (a + d)$, $Q = 6.347–7.463\delta$.[25]

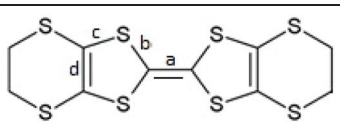

Salt	Donor	*a*/Å	*b*/Å	*c*/Å	*d*/Å	δ	*Q*
I	A	1.368	1.737	1.749	1.361	0.757	0.70^+
	B	1.367	1.741	1.752	1.355	0.771	0.59^+
III	A	1.347	1.744	1.754	1.327	0.824	0.20^+
	B	1.365	1.741	1.760	1.323	0.813	0.28^+
V	A	1.369	1.746	1.758	1.344	0.791	0.44^+
	B	1.352	1.735	1.746	1.340	0.789	0.46^+

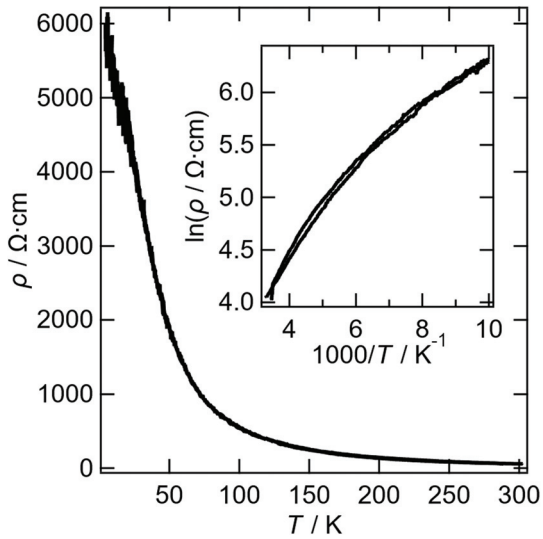

Fig. 7 Resistivity *versus* temperature data for **I**. ln ρ *versus* 1000/*T* inset.

culation of **I** was performed (Fig. S1†). A semi-metal-like Fermi surfaces consisting of hole pockets and quasi-1D electron surfaces were observed. This is the reason why the resistivity curve of **I** does not show linear tendency in the Arrhenius plot. $\rho_{4.2\ K}/\rho_{RT}$ of 104 is much smaller than that of normal semiconductors, suggesting that Fermi surfaces exist in the whole temperature range. In addition, the 1D Fermi surfaces can be nested along the *n* direction ($n = a + b$), where the stronger interactions are observed (r_1–r_3) than those of the other directions. However, the electron surfaces are not straight so that smaller Fermi surfaces still remain after the nesting. The relatively high ρ_{RT} for semimetals suggests that the nesting has already occurred above RT.

Helical crystals of (BEDT-TTF) + [$B_{R/S}$(*S*-mandelate)$_2$] (II)

Electrocrystallisation of BEDT-TTF in the presence of the spiroborate anion synthesised using chiral $B_{R/S}$(*S*-mandelate)$_2^-$ produced helical crystals (**II**). The curved nature of the crystals has meant that X-ray diffraction measurements are not possible (Fig. 8). No crystals could be obtained using the opposite enantiomer $B_{R/S}$(*R*-mandelate)$_2^-$.

The synthesis of the $B_{R/S}$(*S*-mandelate)$_2^-$ anion produces two possible configurations, B_SSS and B_RSS, each adopting very different shapes. The B_SSS anion adopts a 'V' shape and the B_RSS adopts a more planar 'twisted' shape (Fig. 1). Wong *et al.*[25] have stated that 'the twisted anion is favoured by just *ca.* 0.5 kcal mol^{-1} in MeOH over the 'V-shaped' anion, although it is exclusively preferred in the solid state for all salts studied to-date'. Therefore, a possible suggestion for the helical crystals is a preferential crystallisation of the twisted B_RSS anion with the radical-cation BEDT-TTF.

Reproducible four-probe temperature dependent resistivity measurements were made on several crystals of **II** along the long axis of the helix. Salt **II** shows metallic behaviour (ρ_{RT} =

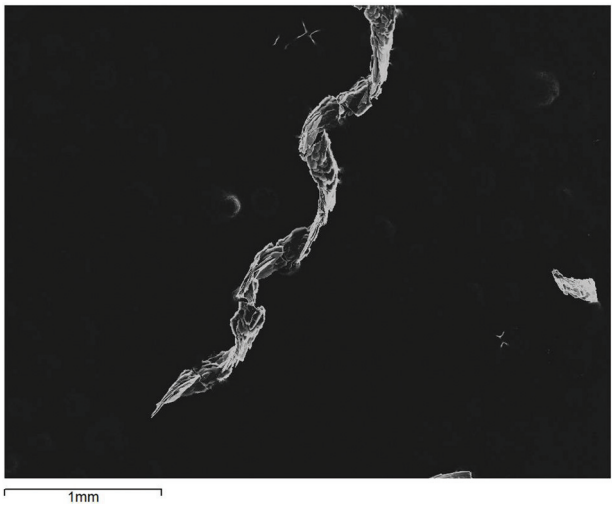

Fig. 8 High resolution 1 mm TEM image of a chiral anti-clockwise helix of **II**.

0.0183 Ω cm) from 300 to 150 K (ρ_{min} = 0.0109 Ω cm) at which point a sharp upturn is observed indicating a metal–insulator transition (Fig. 9). This is in good agreement with the magnetic susceptibility data (Fig. 10) which indicates that a value of 3×10^{-4} emu mol^{-1} is observed for the temperature independent susceptibility from 300 to 150 K at which point the susceptibility decreases with decreasing temperature and becomes zero at 100 K, suggesting a metal–insulator transition at 150 K. From 10 to 2 K the data can be fitted to the Curie–Weiss law with a Curie constant of 0.011 emu K mol^{-1} and a Weiss constant of −0.87 K.

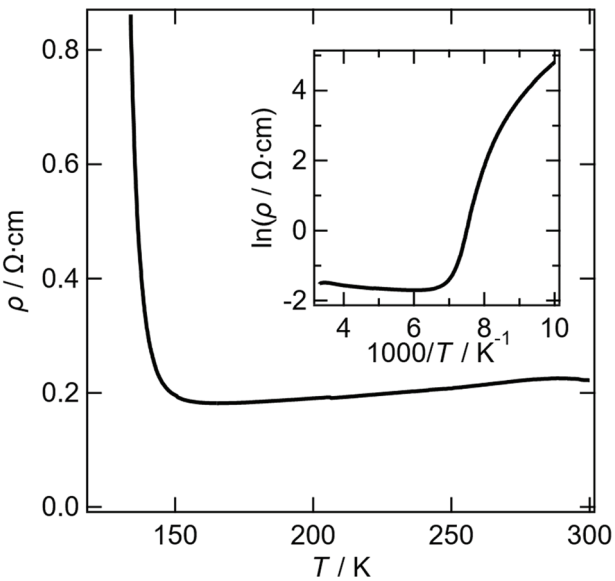

Fig. 9 Resistivity *versus* temperature data for **II**. ln ρ *versus* 1000/T inset.

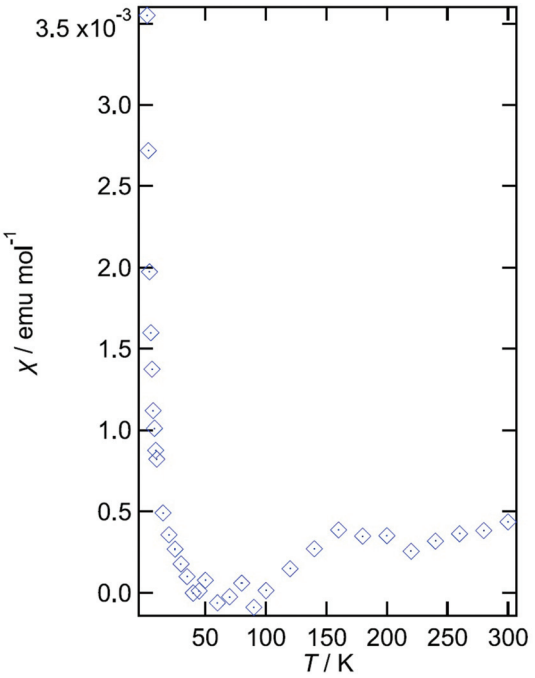

Fig. 10 Magnetic susceptibility of **II**.

δ-(BEDT-TTF)$_2$B$_R$(*R*-2-chloromandelate)$_2$(1,1,2-trichloroethane)$_2$ (III) and δ-(BEDT-TTF)$_2$B$_S$(*S*-2-chloromandelate)$_2$(1,1,2-trichloroethane)$_2$ (IV)

Radical-cation salts **III** and **IV** were synthesised by electrocrystallisation of BEDT-TTF in 1,1,2-trichloroethane (1,1,2-TCE) containing tetraethylammonium spiroborate salts of either *R*- or *S*-2-chloromandelic acid, respectively. Single crystal X-ray diffraction studies show that salts **III** and **IV** are isostructural with the formula δ-(BEDT-TTF)$_2$B$_{R/S}$[(*R*/*S*-2-chloromandelate)$_2$](1,1,2-trichloroethane)$_2$ and crystallise in the non-centrosymmetric space group $P2_12_12$ with a single spiroborate anion, two BEDT-TTF molecules and two 1,1,2-trichloroethane solvent molecules (Fig. 11). Crystals of **IV** were too small (very thin needles) for accurate structural measurement, however, the salt is isostructural with the opposite enantiomer **III**.

Each chiral enantiomer of 2-chloromandelate results in only a single spiroborate enantiomer being present in the crystal structure of the resulting radical-cation salt. This is an example of chiral resolution as the starting spiroborate contains both B$_R$ and B$_S$ enantiomers due to the lability of the boron centre. In the case of *R*-chloromandelate B$_R$ is exclusively present (**III**) and for *S*-chloromandelate the opposite boron enantiomer B$_S$ is the only enantiomer present (**IV**). These two opposite enantiomers conform to the 'V' shaped configuration of the spiroborate which is in contrast to **I** where the more linear 'twisted' configuration is observed in the radical-cation salt. Despite only a minor change in the structure of the anion (the addition of a Cl atom to the phenyl ring of the mandelate) we observe marked differences in the structures of resultant radical-cation salts.

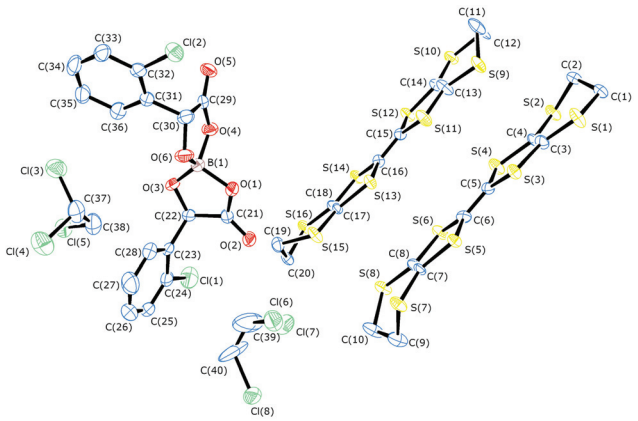

Fig. 11 View showing asymmetric unit contents and atom labelling scheme for **III**. Displacement ellipsoids are drawn at 50% probability level.

In **III** there are two crystallographically independent donors present and they pack in the *bc* plane with neighbouring stacks separated by the insulating anion layer along the *a* direction (Fig. 12). The two independent donors pack in individual side-to-side layers along the *c* direction, whilst in the *b* direction they alternate in an AABBAABB arrangement with each pair of BEDT-TTF donors rotated with respect to each other indicative of *δ* packing (Fig. 13). The AA and BB molecular plane to plane twist angles of 24.9(3)° and 26.7(3)° respectively, and distances of 3.857(4) Å and 3.803(5) Å, between donor pairs, along with the *A* to *B* plane twist angle of 6.5(3)° and distance of 3.465(3) Å, where the AB stacking interaction has only a small deviation from linearity.

The two donors each have side-to-side S···S contacts below the sum of van der Waals radii[28] (Table 3) as well as C–C, H–C and H–S interactions (Table 4).

The spiroborate anions in **III** conform to the so-called V-shape arrangement where the phenyl groups are pointing in the same direction (Fig. 14). A network of short contacts below the sum of VdW radii occur between the anions and adjacent BEDT-TTF molecules as well as 1,1,2-TCE solvent molecules

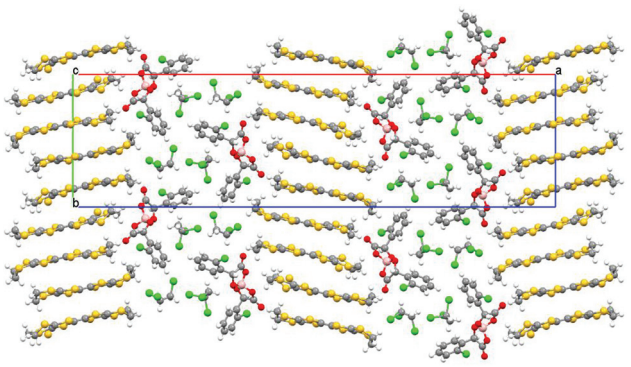

Fig. 12 Layered structure of **III** viewed down the *c* axis.

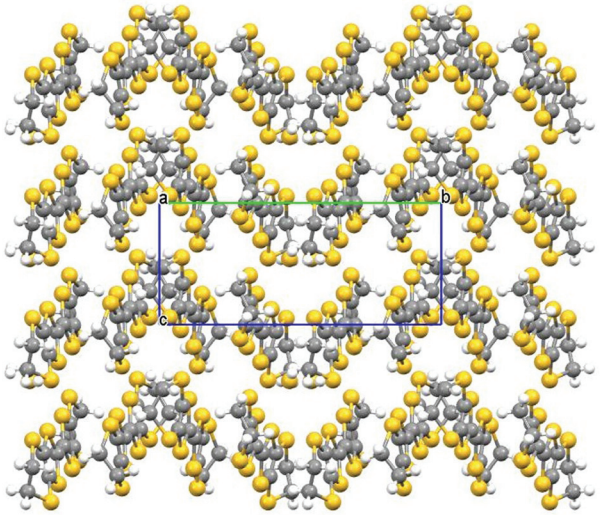

Fig. 13 Donor packing in **III**.

Table 3 S···S contacts shorter than the van der Waals distance for **III**

S···S	Distance/Å	S···S	Distance/Å
S12···S9a	3.377(16)	S1···S4	3.353(3)
S12···S9b	3.491(4)	S5···S8	3.319(3)
S10···S9a	3.370(17)	S7···S8	3.492(4)
S10···S9b	3.442(4)	S1···S2	3.367(4)
S16···S15	3.302(3)		

Table 4 C–H, C–C, Cl–H and C–S short contacts for **III**. Value in square brackets is atom-hydrogen distance

Contact	Distance/Å
C(5)···C(16)	3.377(11)
C(13)···C(2B) [H(2B)]	3.650(13) [2.693]
C16···S13	3.440(3)
S(10)···C(2B) [H(2B)]	3.680(9) [2.904]
S(9B)···C(2B) [H(2B)]	3.810(10) [2.967]
O(5)···S(2)	3.046(6)
O(5)···C(2) [H(2A)]	3.176(11) [2.513]
O(5)···C(9) [H(9A)]	3.213(12) [2.501]
O(2)···C(20) [H(20A)]	3.264(10) [2.341]
S(8)···C(20) [H(20B)]	3.605(9) [2.889]
C(8)···C(20) [H(20B)]	3.632(11) [2.851]
C(7)···C(20) [H(20B)]	3.749(11) [2.884]
C(14)···C(2) [H(2B)]	3.541(12) [2.611]
O(5)···C(1) [H(1A)]	3.671(11) [2.686]
O(2)···S(15)	3.289(6)
O(2)···C(39) [H(39)]	3.118(15) [2.368]
Cl(3)···C(33)	3.427(9) Cl-Pi
Cl(2)···C(29)	3.429(10) Cl-carbonyl

but no considerable interactions appear between anions themselves. The anions stack along the *bc* direction with the carbonyl oxygen, O(5), interacting with BEDT-TTF molecules of the adjacent conducting layer and the phenyl rings of the chloromandelic ligands directed into the centre of the insulating layer.

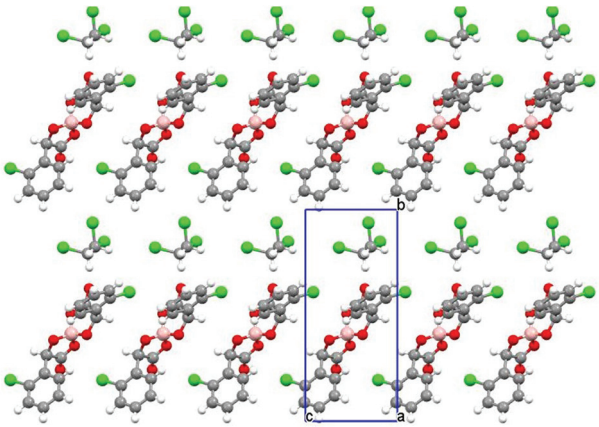

Fig. 14 Anion layer in **III**.

The molecular formula suggests that the two independent donors have a cumulative charge of +1 to balance the charge of the $B_R[R\text{-2-chloromandelate}]_2^-$ anion. Using the method of Guionneau *et al.*[27] for estimating oxidation state from molecular geometry the two donors are calculated as 0.20^+ and 0.28^+. These values are lower than expected which may be due to the higher R factor for this crystal structure. The central C═C bonds are slightly different in length at 1.347(10) (C(5)–C(6)) and 1.367(6) Å (C(15)–C(16)) for independent A and B donors respectively.

Magnetic susceptibility for **III** and **IV** are shown in Fig. 15 and 16, respectively. For **III**, the magnetic susceptibility indicates that it obeys a low dimensional Heisenberg model with J = 20 K, which is 5–10 times smaller than that observed in normal organic conductors having Mott insulating or charge-ordering states where magnetic spins are localised in the donor layers. We will discuss this in the last part of this paragraph. The donor packing arrangement is δ which usually shows semiconducting behaviour and a low dimensional magnetic behaviour. The magnetic interaction J equals to the bandwidth, namely it may have very narrow bands. If so, such narrow bands cannot absorb visible light but absorb only IR light which may explain the golden colour of these crystals.

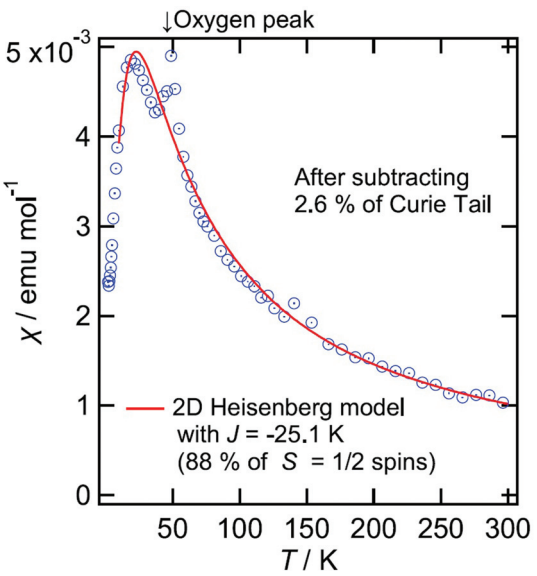

Fig. 15 Magnetic susceptibility of **III**.

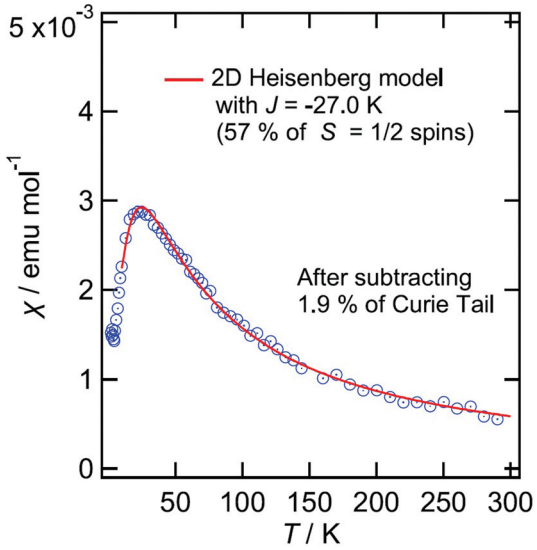

Fig. 16 Magnetic susceptibility of **IV**.

Resistivity measurements could only be measured on a sheet of golden fibres of **III** and of **IV** and so the absolute resistivity is not representative of a single crystal. Semiconducting behaviour is observed for both **III** and **IV** with E_a of 0.113 eV and 0.101 eV, respectively.

Band structure calculations of **III** provide a large Mott gap of 0.155 eV in the band dispersions (Fig. S2†). This indicates that the salts **III** and the isostructural **IV** are Mott insulators. Each donor forms an ABBA tetramer along the stacking direction. However, the interaction between A and B ($p1$) is more than three times stronger than those between A and A ($p3$) and between B and B ($p2$), suggesting that each spin on the AB dimer does not form a spin dimer in the tetramer consisting of two dimers but localized solely on each AB dimer. Therefore, Mott insulating state is dominant rather than band insulating state. The results of the band calculations indicate that the interdimer interactions are weaker than the intradimer interaction and are almost isotropic in the 2D conducting plane (Fig. S2c†). Therefore the magnetic susceptibilities of **III** and **IV** do not obey 1D but obey 2D Hiesenberg models. Usually the BEDT-TTF salts having non-parallel stacking, especially α′- and δ′-type packings, have 1D magnetic structures along the stacking directions and have similar J values of ≈60 K.[29] This means that the side-by-side interactions between adjacent non-parallel stackings are relatively weak. However, the salts **III** and **IV** have 2D magnetic structures according to not only the magnetic behaviours but also the band structures. As mentioned above, $p1$ is more than three times larger than $p2$ and $p3$. The small values of the interdimer interactions

along the stacking directions that are similar to those of the other directions appear to give smaller J values of **III** and **IV**. The reason why $p2$ and $p3$ are relatively small is perhaps because of a large negative pressure caused by the extraordinarily large anion layer consisting of the large anion and trichloroethane molecules.

Experimental

Synthesis and purification of starting materials

BEDT-TTF was purchased from Sigma Aldrich and recrystallised from chloroform. 1,1,2-Trichloroethane, chlorobenzene *R*-(−)-mandelic acid, *S*-(+)-mandelic acid, mandelic acid, *R*-(−)-2-chloromandelic acid, *S*-(+)-2-chloromandelic acid, 2-chloromandelic acid, boric acid, sodium hydroxide, triethylamine and 18-crown-6 were purchased from Sigma Aldrich and used as received.

Synthesis of K[B(mandelate)$_2$]

Boric acid (0.62 g, 10.0 mmol, 1.00 equiv.) was added to a solution of mandelic acid (3.04 g, 20.0 mmol, 2.00 equiv.) in water (30 ml). To this was added a solution of potassium hydroxide (0.58 g, 10.0 mmol, 1.00 equiv.) in water (30 ml) and the reaction mixture heated to reflux for 8 hours. The white powder obtained was recrystallised twice from water and once from ethanol. The same method was used replacing mandelic acid with either *R*-(−)-mandelic acid or *S*-(+)-mandelic acid. Yields of ~85% were obtained in all cases.

Data for K[B$_{R/S}$(*R*-mandelate)$_2$] ^{1}H NMR (400 MHz, CD_3CN) δ ppm 5.17 (s, 0.4 H, *chiral*), 5.20 (s, 1.6 H, *chiral*), 7.26–7.32 (m, 2 H), 7.34–7.41 (m, 4 H), 7.49–7.59 (m, 4H).

Data for K[B$_{R/S}$(*S*-mandelate)$_2$] ^{1}H NMR (400 MHz, CD_3CN) δ ppm 5.17 (s, 1 H, *chiral*), 5.20 (s, 1 H, *chiral*), 7.25–7.32 (m, 2 H), 7.33–7.42 (m, 4 H), 7.50–7.58 (m, 4 H).

Synthesis of [NEt$_3$H][B(2-chloromandelate)$_2$]

S- or *R*-2-chloromandelic acid (0.94 g, 5 mmol) was added to a solution of boric acid (0.16 mg, 2.5 mmol) and triethylamine (2 mL, 10 mmol) in toluene (50 mL) and heated to reflux for 4 hours. The supernatant was removed *in vacuo* resulting in a clear pale yellow oil of [NEt$_3$H][B$_{R/S}$(2-chloromandelate)$_2$] (1.10 g, 92%) which was used without further purification.

Data for [HNEt$_3$][B$_{R/S}$(*S*-2-chloromandelate)$_2$] ^{1}H NMR (400 MHz, DMSO-d_6) δ ppm 1.15 (t, J = 7.32 Hz, 9 H), 3.07 (q, J = 7.32 Hz, 6 H), 5.53 (s, 1 H, *chiral*), 5.56 (s, 1 H, *chiral*), 7.10–7.48 (m, 8 H), 7.57–7.65 (m, 2 H).

Data for [HNEt$_3$][B$_{R/S}$(*R*-2-chloromandelate)$_2$] ^{1}H NMR (400 MHz, DMSO-d_6) δ ppm 1.15 (t, J = 7.20 Hz, 9 H), 3.07 (q, J = 7.17 Hz, 6 H), 5.52 (s, 1 H, *chiral*), 5.55 (s, 1 H, *chiral*), 7.25–7.51 (m, 6 H), 7.56–7.65 (m, 2 H).

Synthesis of radical-cation salts

Crystals of **I–IV** were grown on platinum electrodes by electrocrystallisation in 40 ml H-shaped electrochemical cells.

Platinum electrodes were cleaned by applying a voltage across the electrodes in 1 M H_2SO_4 in each direction to produce H_2 and O_2 at the electrodes, then washed with distilled water and thoroughly dried.

(I)

K[B$_{R/S}$(*R*/*S*-mandelate)$_2$] (100 mg) and 18-crown-6 (200 mg) were dissolved in chlorobenzene (30 ml) with stirring overnight before filtering into an H-cell containing BEDT-TTF (10 mg) in the anode compartment. H-Cells were placed in a dark box on a vibration-free bench at a constant current of 0.2 μA and after 21 days a large number of very thin black plates were harvested from the anode.

(II)

K[B$_{R/S}$(*S*-mandelate)$_2$] (100 mg) and 18-crown-6 (200 mg) were dissolved in chlorobenzene (10 ml) and ethanol (1 ml) with stirring overnight before filtering into an H-cell containing BEDT-TTF (10 mg) in the anode compartment. H-Cells were placed in a dark box on a vibration-free bench at a constant current of 0.2 μA and after 21 days a large number of macromolecular crystalline helices were harvested from the anode. Attempts to grow crystals using other solvents proved unsuccessful. Despite repeated attempts using a variety of conditions it was not possible to obtain single crystals using the opposite enantiomer.

(III)

[NEt$_3$H][B$_{R/S}$(*S*-2-chloromandelate)$_2$] (104 mg) was dissolved in 1,1,2-TCE (40 mL) with stirring overnight before filtering into an H-cell containing BEDT-TTF (10 mg) in the anode compartment. H-Cells were placed in a dark box on a vibration-free bench at a constant current of 0.3 μA. After 15 days thin gold needles of were harvested from the anode.

(IV)

[NEt$_3$H][B$_{R/S}$(*R*-2-chloromandelate)$_2$] (95 mg) was dissolved in 1,1,2-TCE (40 mL) with stirring overnight before filtering into an H-cell containing BEDT-TTF (10 mg) in the anode compartment. H-Cells were placed in a dark box on a vibration-free bench at a constant current of 0.3 μA. After 15 days thin gold needles were harvested from the anode.

Physical measurements

Four-probe DC transport measurements were made on crystals using a HUSO HECS 994C multi-channel conductometer. Gold wires (15 μm diameter) were attached to the crystal, and the attached wires were connected to an integrated circuit plug with carbon conductive cement. For **III** and **IV** four Au wires are attached on a sheet of golden fibres.

Magnetic susceptibility measurements were performed with a Quantum Design MPSM2 SQUID magnetometer using randomly orientated polycrystalline material encased in aluminium foil.

Conclusions

Four new radical-cation salts of BEDT-TTF with $B(mandelate)_2^-$ or $B(2\text{-chloromandelate})_2^-$ have been synthesised. The salts have novel packing arrangements of the $B(mandelate)_2^-$ or $B(chloromandelate)_2^-$ anions and show preference for certain diastereomers or enantiomers over others in the electrochemical synthesis. Radical-cation salts displaying a macromolecular helical morphology have not been observed before, as seen here when using enantiopure ligands on the spiroborate anion. We have synthesised a library of spiroborate anions with chiral ligands and we continue to synthesise further radical-cation salts of BEDT-TTF to explore the effect of chirality upon conductivity.

Conflicts of interest

There are no conflicts to declare.

Acknowledgements

LM and TJB would like to thank the Royal Society and Leverhulme Trust for financial support (LT170022 and RPG-2019-242). JRL and LM thank NTU for a PhD studentship. We thank EPSRC for funding the National Crystallography Service.

Notes and references

1 J. M. Williams, J. R. Ferraro, R. J. Thorn, K. D. Carlson, U. Geiger, H. H. Wang, A. M. Kini and M. H. Whangbo, *Organic Superconductors: Synthesis, Structure, Properties and Theory*, Prentice Hall, Englewood Cliffs, NJ, 1992.

2 N. Avarvari and J. D. Wallis, *J. Mater. Chem.*, 2009, **19**, 4061.

3 G. L. J. A. Rikken and E. Raupach, *Nature*, 1997, **390**, 493; G. L. J. A. Rikken, J. Folling and P. Wyder, *Phys. Rev. Lett.*, 2001, **87**, 236602.

4 V. Krstic, S. Roth, M. Burghard, K. Kern and G. L. J. A. Rikken, *J. Chem. Phys.*, 2002, **117**, 11315; V. Krstic and G. L. J. A. Rikken, *Chem. Phys. Lett.*, 2002, **364**, 51; G. L. J. A. Rikken, *Science*, 2011, **331**, 864.

5 F. Pop, P. Auban-Senzier, E. Canadell, G. L. J. A. Rikken and N. Avarvari, *Nat. Commun.*, 2014, **5**, 3757, DOI: 10.1038/ncomms4757; F. Pop, P. Auban-Senzier, A. Frackowiak, K. Ptaszyński, I. Olejniczak, J. D. Wallis, E. Canadell and N. Avarvari, *J. Am. Chem. Soc.*, 2013, **135**, 17176–17186.

6 F. Pop, P. Auban-Senzier, A. Frackowiak, K. Ptaszynski, I. Olejiniczak, J. D. Wallis, E. Canadell and N. Avarvari, *J. Am. Chem. Soc.*, 2013, **135**, 17176–17186.

7 J. D. Dunitz, A. Karrer and J. D. Wallis, *Helv. Chim. Acta*, 1986, **69**, 69.

8 I. Awheda, S. Krivickas, S. Yang, L. Martin, M. A. Guziak, A. C. Brooks, F. Pelletier, M. Le Kerneau, P. Day, P. Horton, H. Akutsu and J. D. Wallis, *Tetrahedron*, 2013, **69**, 8738; S. J. Krivickas, C. Hashimoto, J. Yoshida, A. Ueda, K. Takahashi, J. D. Wallis and H. Mori, *Beilstein J. Org. Chem.*, 2015, **11**, 1561; F. Leurquin, T. Ozturk, M. Pilkington and J. D. Wallis, *J. Chem. Soc., Perkin Trans. 1*, 1997, 3173–3178.

9 F. Riobé and N. Avarvari, *Chem. Commun.*, 2009, 3753.

10 J. Lieffrig, R. Le Pennec, O. Jeannin, P. Auban-Senzier and M. Fourmigué, *CrystEngComm*, 2013, **15**, 4408.

11 S. Yang, A. C. Brooks, L. Martin, P. Day, H. Li, P. Horton, L. Male and J. D. Wallis, *CrystEngComm*, 2009, **11**, 993.

12 M. Chas, M. Lemarié, M. Gulea and N. Avarvari, *Chem. Commun.*, 2008, 220; M. Chas, F. Riobé, R. Sancho, C. Minguillón and N. Avarvari, *Chirality*, 2009, **21**, 818.

13 L. Martin, J. D. Wallis, M. A. Guziak, J. Oxspring, J. R. Lopez, S.-i. Nakatsuji, J.-i. Yamada and H. Akutsu, *CrystEngComm*, 2014, **16**, 5424.

14 J. Short, T. J. Blundell, S. Krivickas, S. Yang, J. D. Wallis, H. Akutsu, Y. Nakazawa and L. Martin, *Chem. Commun.*, 2020, **56**, 9497–9500.

15 E. Coronado, S. Curreli, C. Giménez-Saiz, C. J. Gómez-García, P. Deplano, M. L. Mercuri, A. Serpe, L. Pilia, C. Faulmann and E. Canadell, *Inorg. Chem.*, 2007, **46**(11), 4446–4457.

16 A. M. Madalan, E. Canadell, P. Auban-Senzier, D. Brânzea, N. Avarvari and M. Andruh, *New J. Chem.*, 2008, **32**, 333–339.

17 E. Coronado, J. R. Galan-Mascaros, C. J. Gomez-Garcıa, A. Murcia-Martınez and E. Canadell, *Inorg. Chem.*, 2004, **43**, 8072–8077.

18 F. Riobé, F. Piron, C. Réthoré, A. M. Madalan, C. J. Gómez-García, J. Lacour, J. D. Wallis and N. Avarvari, *New J. Chem.*, 2011, **35**, 2279–2286.

19 M. Atzori, F. Pop, P. Auban-Senzie, C. J. Gómez-García, E. Canadell, F. Artizzu, A. Serpe, P. Deplano, N. Avarvari and M. L. Mercuri, *Inorg. Chem.*, 2014, **53**(13), 7028–7039.

20 M. Atzori, F. Pop, P. Auban-Senzier, R. Clérac, E. Canadell, M. L. Mercuri and N. Avarvari, *Inorg. Chem.*, 2015, **54**(7), 3643–3653.

21 S. Rashid, S. S. Turner, P. Day, M. E. Light and M. B. Hursthouse, *Inorg. Chem.*, 2000, **39**(11), 2426–2428.

22 L. Martin, *Coord. Chem. Rev.*, 2018, **376**, 277–291; S. Benmansour and C. J. Gómez-García, *Magnetochemistry*, 2021, **7**(7), 93.

23 M. Kurmoo, A. W. Graham, O. Day, S. J. Coles, M. B. Hursthouse, J. L. Caulfield, J. Singleton, F. L. Pratt, W. Hayes, L. Ducasse and P. Guionneau, *J. Am. Chem. Soc.*, 1995, **117**, 12209; L. Martin, S. S. Turner, P. Day, F. E. Mabbs and E. J. L. McInnes, *Chem. Commun.*, 1997, 1367–1368; L. Martin, S. S. Turner, P. Day, K. M. Abdul Malik, S. J. Coles and M. B. Hursthouse, *Chem. Commun.*, 1999, 513–514.

24 J. R. Lopez, L. Martin, J. D. Wallis, H. Akutsu, Y. Nakazawa, J.-i. Yamada, T. Kadoya, S. J. Coles and C. Wilson, *Dalton Trans.*, 2016, **45**, 9285–9293.

25 L. W.-Y. Wong, J. W.-H. Kan, T. Nguyen, H. H.-Y. Sung, D. Li, A. S.-F. Au Yeung, R. Sharma, Z. Lin and I. D. Williams, *Chem. Commun.*, 2015, **51**, 15760–15763.
26 T. J. Blundell, M. Brannan, H. Nishimoto, T. Kadoya, J.-i. Yamada, H. Akutsu, Y. Nakazawa and L. Martin, *Chem. Commun.*, 2021, **57**, 5406–5409.
27 P. Guionneau, C. J. Kepert, D. Chasseau, M. R. Truter and P. Day, *Synth. Met.*, 1997, **86**, 1973.
28 S. S. Batsanov, *Inorg. Mater.*, 2001, **37**, 871.
29 S. D. Obertelli, R. H. Friend, D. R. Talham, M. Kurmoo and P. Day, *J. Phys.: Condens. Matter*, 1989, **1**, 5671–5680; M. Kurmoo, M. Allan, R. Friend, D. Chasseau, G. Bravic and P. Day, *Synth. Met.*, 1994, **41–43**, 2127–2130; T. Mallah, C. Hollis, S. Bott, M. Kurmoo, P. Day, M. Allan and R. H. Friend, *J. Chem. Soc., Dalton Trans.*, 1990, 859–865; H. Akutsu, K. Ishihara, S. Ito, F. Nishiyama, J.-i. Yamada, S.-i. Nakatsuji, S. S. Turner and Y. Nakazawa, *Polyhedron*, 2017, **136**, 23–29; H. Akutsu, A. Kohno, S. S. Turner and Y. Nakazawa, *Chem. Lett.*, 2020, **49**(11), 1345–1348.
30 *CrysAlisPRO*, Oxford Diffraction/Agilent Technologies UK Ltd, Yarnton, England.